Electric fields and dominant carrier transport mechanisms in CdTe Schottky detectors

Adriano Cola and Isabella Farella
Institute for Microelectronics and Microsystems – Unit of Lecce, National Council of Research (IMM/CNR), Lecce I-73100, Italy

(Received 11 December 2012; accepted 7 March 2013; published online 19 March 2013)

CdTe Schottky diodes for X- and γ-ray detection exhibit excellent spectroscopic performance, even though these are not stable under operative voltages. Improvements require the comprehension of the main carrier transport mechanisms, presently unclear. We address this issue by correlating the internal electric field and the flowing current. Depending on the temperature and applied voltage, different mechanisms become dominant where the deep levels always play a central role. Indeed, the partial ionization of deep levels directly controls the electric field distribution. Transient measurements show how, under high voltages, the field at the contacts controls the current flowing through the detector. © *2013 American Institute of Physics*. [http://dx.doi.org/10.1063/1.4795942]

Understanding charge carrier transport in radiation detectors is of extreme relevance as detectors rely on the efficient collection of photo-generated charge pairs. High electric fields over several mm thickness with low leakage current levels are basic requirements for efficiently detecting X- and γ-photons, and this involves the use of semi-insulating (SI) materials and suitable contacts. In this regard, Schottky detectors based on high quality SI CdTe have been produced: they sustain high operating voltages with sufficiently low currents and show excellent spectroscopic performance.[1] However, transient phenomena known as *bias induced polarization* seriously degrade their operation: under bias, a space charge builds up which eventually shrinks the electric field under the blocking contact.[2] Additionally, the current exhibits non monotonic transients, as recently published by Principato *et al*.[3] Focusing on detector behaviour, only empirical methods, such as temperature decreasing[1] or bias resetting[4] have been devised to limit the bias induced polarization. These reflect the large number of open issues on the material side, such as the homogeneity or the bulk compensation mechanism,[5,6] and on the detector fabrication side, such as the role of interface layers between contacts and the CdTe. It is worth to remind that under high radiation flux, Cd(Zn)Te detectors also experience a reduction of counting rate and spectroscopic performance with time. This *radiation induced polarization*, still related to a space charge build-up, is additionally characterized by a progressive decrease of the carrier lifetime.[7]

Within the sketched framework, the spatial distribution of the electric field within the detectors is crucial to understand the mechanisms which are ultimately responsible for the bias induced polarization. The electric field and the flowing current provide the basic ingredients for the description of carrier transport, i.e., Poisson and current equations, with the proper boundary conditions given by the contacts.

The aim of this letter is to contribute to the understanding of the basic properties of CdTe Schottky detectors, correlating measurements of current and electric field as a function of applied voltage, and temperature, particularly in transient regimes. Pockels effect has been used to probe the spatial/temporal distribution of the electric field. This effect has shown to be very effective when applied to CdTe detectors,[8–11] due to the large electro-optic coefficient and to the limited perturbation of the field itself. In the experiments, we have used the crossed polariser technique where linearly polarised near infrared radiation (NIR) impinges perpendicular to the lateral surface of the detector, thus parallel to the contacts. By passing through the detector, the radiation experiences the birefringence induced in the crystal by the applied voltage and is detected after crossing a second polariser whose axis is perpendicular to the first one. The transmitted probe intensity is digitized by a charge coupled device with enhanced sensitivity in the NIR range equipped with a 6× zoom lens and stored as an image. For each (x, y) projection point of the detector side, the intensity $I(x, y)$ of the transmitted light depends on the electric field distribution $E(x, y)$ averaged along the optical path (z-direction), through the relation[12]

$$I(x,y) = I_0(x,y)\sin^2\left[\frac{\pi}{2}\frac{E(x,y)}{E_0}\right], \tag{1}$$

where $I_0(x,y)$ is the transmitted intensity with both the polarisers parallel. The constant E_0 depends on material properties and size, and on the wavelength of the probe radiation, which is 980 nm in our case. The electric field profile $E(y)$ from anode to cathode is calculated by averaging $E(x,y)$ along the x-direction, parallel to the electrodes. The radiation wavelength has been selected from a tungsten source by a narrow band filter (FWHM = 10 nm); the intensity has been kept as low as possible, and it was verified that the probe radiation did not affect at all the E-field distribution and, only weakly, the measured current. Measurements have been carried out at different temperatures from 25 °C to 60 °C (stability ± 0.1 °C). Details on the experimental setup have been previously published.[9] Both voltage sweeps (up to 900 V, in steps of 10 V) and transients experiments (sampling time $\Delta t = 1$ s) at fixed voltage have been performed using a source-monitor unit while simultaneously recording Pockels images. In the voltage sweeps, data acquisition occurs 1 s after each staircase voltage step is applied. It is evident that measurements carried out during the voltage sweeps are not stationary but they approximately correspond to the first sampling data acquired during transients at fixed bias.

For transient measurements (at 600 V), data acquisition starts at the end of the upward voltage staircase (step 10 V).

Measurements refer to an Acrorad planar detector 10×10 mm^2 in size, 1 mm thick, but similar results have been found on other nominally equal detectors. The material is a high quality (111)-oriented Cl doped SI (resistivity $\sim 10^9\,\Omega\,$cm), slightly *p*-type CdTe single crystal, grown by Traveling Heater Method. The anode contact is formed by depositing In on the Te-face of the crystal, followed by a Ti layer; the Pt contact, electroless deposited on the Cd-rich opposite face, acts as a cathode. Polariser and analyser are oriented at 45° and −45°, respectively, with respect to the (111) crystal direction along which the external electric field is applied.

The electric field profiles obtained during the voltage sweeps at T = 25 °C are reported in Fig. 1.

According to what happens in a Schottky barrier on a *p*-type semiconductor, the field linearly drops from anode to cathode with a slope almost independent of the applied voltage. From Poisson equation, the field slope corresponds to a negative space charge ranging from 1.5×10^{11} to 2.5×10^{11} cm^{-3}. We remind here that the semi-insulating behaviour in CdTe is achieved by means of the partial ionization of deep levels which compensate shallow levels.[6] Applying a reverse bias to the blocking contact causes a depletion of free holes and a consequent increase of the deep level ionization. The linearity of the electric field is indicative of the uniformity of the ionization across the detector. As it can be seen in Fig. 2 the ionization strongly depends on the temperature, to such an extent that the space charge increases of about one order of magnitude from 25 to 60 °C (see inset graph). As a consequence, for T > 50 °C the field becomes negligible near the cathode when a 600 V voltage is applied.

Hence, at each temperature, during the voltage sweeps, there exists a critical voltage value V_c at which the field starts to become not negligible near the cathode. For tested temperatures, these values have been reported in Fig. 3 and highlighted along the corresponding current-voltage (I-V) curves.

At low voltages, the current follows a $I \propto V^{1/2}$ power law behaviour, which tends to become quadratic under high voltages. It could seem, therefore, that for low voltages, the current is due to the blocked holes, while electrons injected from the (Ohmic) cathode prevail when the electric field near the cathode is no longer negligible.[13] Consistently, the transition between the two mechanisms occurs at about V_c.

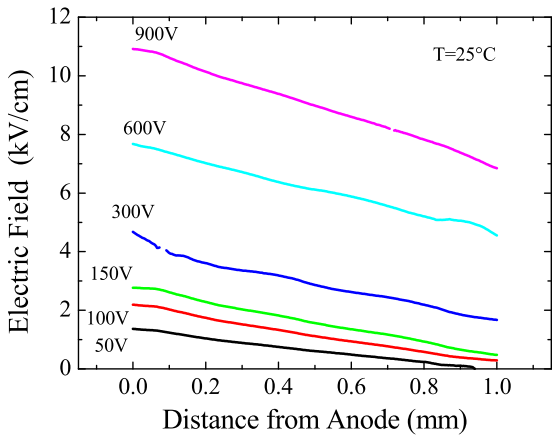

FIG. 1. Electric field profiles for different applied voltages at T = 25 °C.

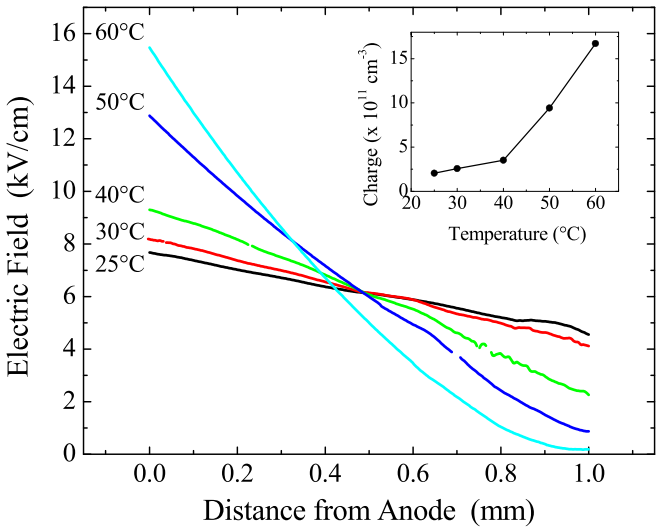

FIG. 2. Electric field profiles at 600 V for tested temperatures: T = (25, 30, 40, 50, 60) °C. Inset graph refers to the calculated space charge at the anode.

Theoretically, an ideal reverse biased diode is expected to show a saturated current; for a real diode, a relation $I \propto \exp(V^n)$ is expected, where $n < 1$ depends on the specific carrier transport mechanism[14] (e.g., interface layer and Schottky effect). Measurements at low voltages reported in Fig. 3 do show neither the saturated current nor the exponential law. In agreement with Kosyachenko *et al.*,[15] thermal carrier generation in the *partially* depleted region can rather be the dominant mechanism: the measured current grows indeed with the observed extension of the depletion region, i.e., as $V^{1/2}$, like in a standard Schottky junction. Moreover, when the depletion width equals the entire detector thickness, the generation current becomes

$$J = q\int_0^w G dx \overset{w=L}{=} q \cdot G \cdot L, \tag{2}$$

where it is assumed that the generation rate G is constant throughout the depletion region. Hence, the thermal

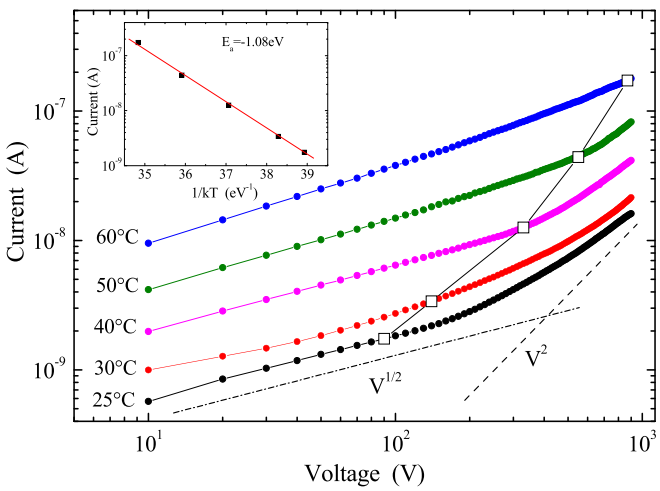

FIG. 3. I-V characteristics at different temperatures. Current points corresponding to critical V_c voltages are also highlighted (linked squares). Also plotted the lines corresponding to the root squared (dot dash) and quadratic (dash) laws. In the inset, Arrhenius plot of the current values corresponding to V_c (activation energy $E_a = -1.08$ eV).

dependence of J is only contained in G which shows, according to the standard Shockley-Read-Hall expression,[16] an activation energy function of the carrier generation centre properties (energy level, carrier capture coefficients), and of the free electron-hole concentrations, when not negligible. By considering, for each temperature, the current values corresponding to V_c, i.e., for $w = L$, the predicted exponential behaviour is obtained, see inset graph in Fig. 3. This further confirms that at low voltages ($V < V_c$), the dominant mechanism is the thermal carrier generation. From data fitting, an activation energy equal to $E_a = -1.08$ eV is obtained.

The electron contribution to the current at high voltages is elucidated by the transient measurements. Indeed, the electric field shows pronounced, temperature-dependent transients: the field increases at the anode and (in general) decreases at the cathode. A strong correlation between field transients at the contacts and the corresponding flowing current is noticed: at 25 °C and 30 °C, the current transients closely resemble the behaviour of the field at the cathode (Figs. 4(a) and 4(b)). As the temperature increases, the field at the cathode eventually becomes negligible. At T = 40 °C (Fig. 4(c)) when it becomes as small as few hundreds V/cm (t ≈ 200 s), the current suddenly stops decreasing and starts to increase. This behaviour is also observed for T = 50 °C (Fig. 4(d)) but at a shorter time, t ≈ 50 s. For T = 60 °C (Fig. 4(e)), the field is already negligible at the cathode at the transient beginning (t = 0), and the current shows only an increasing behaviour, matching the field at the anode (see Fig. 4(f)). The correlations observed between the field at cathode and the current transients evidence the role played by the Ohmic contact in such detectors: whenever the field at (or very close to) the Ohmic contact is not negligible, electrons will be injected, and drifted away by the field, determining in this way the main contribution to the flowing current. The electron injection mechanism has been already pointed out in the quadratic behaviour seen in Fig. 2. Current transients in Schottky CdTe detectors are thus strictly related to the electric field near the contacts: if the electric field at the cathode decreases with time, it gives rise to an (electron) current which decreases, too.

On the other hand, the transient increase in the current, dominant at high temperatures, has to be connected to the considerable field enhancement at the anode (Fig. 4(f)) when the field is negligible at the cathode. The electric field transients at the anode show high values at high temperatures and a clear thermal activation. In such case, thermal generation cannot be the dominant mechanism, as the current increases while the depletion region shrinks. As previously reported for similar experimental conditions, the field-dependent barrier height at the metal/semiconductor interface can be attributed to the presence of an interfacial layer.[2,17] The relation between the current I and the field at the anode E_{ano} is given, in this case, by

$$I(t) = I_0 e^{q\alpha E_{ano}(t)/k_B T}, \tag{3}$$

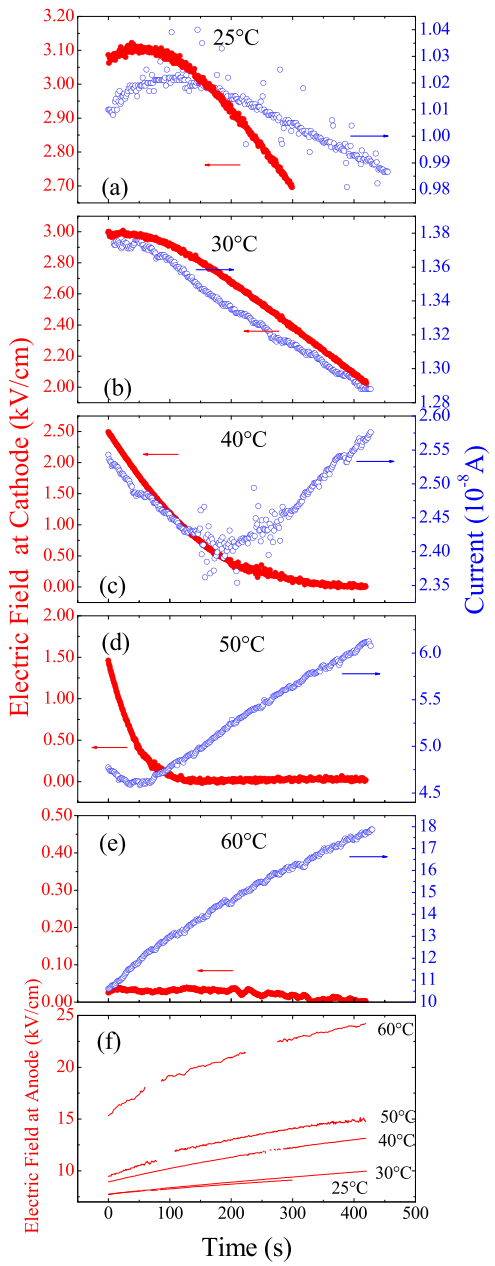

FIG. 4. From (a) to (e) transients of the current (empty circles, blue on-line) and of electric field (full circles, red on-line) at the cathode, for T = (25, 30, 40, 50, 60) °C; (f) transients of the electric field at the anode, for the same temperatures. All data refer to 600 V.

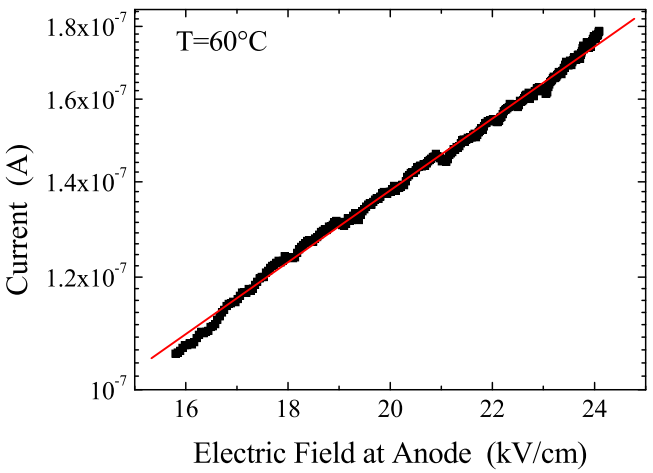

FIG. 5. Current transient data at 600 V and T = 60 °C plotted as a function of the corresponding field at the anode. Line represents data fit using Eq. (3).

where I_o is a constant and α is the interfacial layer thickness. In Fig. 5, which refers to $T = 60\,^{\circ}C$, the semilog plot of I vs. E_{ano} follows relation (3). This gives indications that the barrier reduction is so large that the thermionic hole emission across the Schottky barrier becomes the main carrier transport mechanism. An interface layer thickness of 17 nm has been estimated from data fitting. It has to be mentioned that such a thickness is too large to activate the tunnelling mechanism through an insulating interfacial layer.[18] On the other hand, a thick and complex interface has been reported between In and CdTe.[19] Hence, our results indicate that Eq. (3) can be still applied, but the meaning of α coefficient is unclear.

At lower temperatures, $T = 50\,^{\circ}C$ and $T = 40\,^{\circ}C$, relation (3) is also verified for that portion of the current transients showing increasing values.

To conclude, we have shown that different carrier transport mechanisms compete in CdTe Schottky detectors: at low voltages, thermal generation dominates, while at high voltages, electron injection from the Pt Ohmic contact prevails. Thermally activated field transients are always present, and they tend to shrink the electric field near the anode. If this occurs when voltage bias is sufficiently high, the holes, emitted across the reduced barrier at the anode, become dominant. Clearly a strongly non-uniform electric field degrades detector performance. However, in Schottky CdTe detectors, the space charge build-up *always* takes place because of the presence of deep levels and of the hole depletion. Low temperature and high bias can only limit such effect.

Finally, it is worth noticing that the Ohmic cathode causes, under operative voltages, a large current level (quadratic with the voltage), which represents a detrimental and relevant source of noise in the detector. At the same time, it provides an electron excess into the bulk, which can indirectly contribute to the increase of the negative space charge and hence to the bias induced polarization.

The authors thank Dr. Alessandra S. Lanotte for stimulating exchanges.

[1]T. Takahashi, T. Mitani, Y Kobayashi, M. Kouda, G. Sato, S. Watanabe, K. Nakazawa, Y. Okada, M. Funaki, R. Ohno, and K. Mori, IEEE Trans. Nucl. Sci. **49**, 1297 (2002).
[2]A. Cola and I. Farella, Appl. Phys. Lett. **94**, 102113 (2009).
[3]F. Principato, G. Gerardi, A. A. Turturici, and L. Abbene, J. Appl. Phys. **112**, 094506 (2012).
[4]T. Seino, S. Kominami, Y. Ueno, and K. Amemiya, IEEE Trans. Nucl. Sci. **55**(5), 2770 (2008).
[5]N. Krsmanovic, K. G. Lynn, M. H. Weber, R. Tjossem, Th. Gessmann, Cs. Szeles, E. E. Eissler, J. P. Flint, and H. L. Glass, Phys. Rev. B **62**, R16279 (2000).
[6]M. Fiederle, C. Eiche, M. Salk, R. Schwarz, K. W. Benz, W. Stadler, D. M. Hofmann, and B. K. Meyer, J. Appl. Phys. **84**, 6689 (1998).
[7]D. S. Bale and C. Szeles, Phys. Rev. B **77**, 035205 (2008).
[8]A. Zumbiehl, M. Hage-Ali, P. Fougeres, J. M. Koebel, R. Regal, and P. Siffert, J. Cryst. Growth **197**, 650 (1999).
[9]A. Cola, I. Farella, A. M. Mancini, and A. Donati, IEEE Trans. Nucl. Sci. **54**(4), 868 (2007).
[10]P. J. Sellin, G. Prekas, J. Franc, and R. Grill, Appl. Phys. Lett. **96**, 133509 (2010).
[11]J. Franc, V. Dědič, P. J. Sellin, R. Grill, and P. Veeramani, Appl. Phys. Lett. **98**, 232115 (2011).
[12]S. Namba, J. Opt. Soc. Am. **51**, 76 (1961).
[13]M. A. Lampert, Phys. Rev. **103**, 1648 (1956).
[14]E. H. Rhoderick and R. H. Williams, *Metal-Semiconductor Contacts* (Clarendon, Oxford, 1988).
[15]L. A. Kosyachenko, O. L. Maslyanchuk, V. A. Gnatyuk, C. Lambropoulos, I. M. Rarenko, V. M. Sklyarchuk, O. F. Sklyarchuk, and Z. I. Zakharuk, Semicond. Sci. Technol. **23**, 075024 (2008).
[16]W. Shockley and W. T. Read, J. Phys. Rev. **87**, 835 (1952).
[17]H. Toyama, A. Higa, M. Yamazato, T. Maehama, R. Ohno, and M. Toguchi, Jpn. J. Appl. Phys., Part 1 **45**, 8842 (2006).
[18]H. C. Card and E. H. Rhoderick, J. Phys. D: Appl. Phys. **4**, 1602 (1971).
[19]K. Okada, H. Yasufuku, H. Yoshikawa, and Y. Sakurai, Appl. Phys. Lett. **92**, 073501 (2008).